

**Characterization of Amchitka Island Subsurface: Ground  
Water Modeling in the Vicinity of the Long Shot Test Shot**

June 17, 2005

Anna Forsstrom and David L. Barnes  
Water & Environmental Research Center, Department of Civil and  
Environmental Engineering, University of Alaska Fairbanks

Executive Summary .....	1
1. Introduction .....	2
1.1. Geology .....	2
1.1.1. Geology of the Long Shot site .....	3
1.2. Hydrology .....	4
1.2.1. Hydrology of the Long Shot site .....	5
1.3. Freshwater saltwater interface.....	7
1.4. Previous ground water models of Long Shot.....	8
2. Methodology .....	9
2.1. Geometry and boundary conditions of the model .....	9
2.2. Base-case parameters.....	10
2.3. Calibration of the model.....	10
2.3.1. Scenarios investigated .....	11
2.3.2. Recharge and hydraulic conductivity .....	11
2.3.3. Transverse and longitudinal dispersivities .....	12
3. Results.....	12
3.1. Calibration to magnetotelluric data .....	12
3.1.1. Homogeneous .....	12
3.1.2. Andesite sills influence on the ground water flow .....	17
4. Discussions and conclusions .....	20
Appendix A .....	23
Appendix B .....	26
References .....	29

## EXECUTIVE SUMMARY

The objective of this study is to characterize the ground-water flow through the basin in which the Long Shot test was conducted. To meet this objective a two-dimensional ground-water flow model of a cross section through the Long Shot site was developed. This model incorporated values from literature data and magnetotelluric (MT) data taken summer 2004. Using these data sources several likely scenarios were investigated and the results were compared to the results obtained in past modeling efforts conducted by others (DRI, 2002; Wheatcraft, 1995; and Fenske, 1972).

Ground-water flow through two different representations of the fractured rock's hydraulic conductivity was modeled. The first approach was to assume that the hydraulic conductivity was homogeneous as was done in the DRI study (2002). Given the evidence of a more permeable layer (andesite sills) in the basin at approximately the same depth as the Long Shot working point, the second approach included these sills in the model. Values for likely hydraulic conductivity were obtained from literature (US Army Corp of Engineers and USGS, 1965; Gard and Hale, 1964). A reported value of average annual precipitation and possible range of recharge were also obtained from literature (Merritt and Fuller, 1977; Gard and Hale, 1964). For each scenario investigated, the parameters were adjusted such that the extent of the transition zone determined through modeling matched the depths determined in the MT survey.

The best comparison between the spatial distribution of the upper transition zone obtained from modeling to the distribution measured by MT is obtained when the andesite sills are included. Even though additional work is required on these scenarios to obtain a better fit to the MT results, this results does indicate that the sills do influence the ground-water flow. In these scenarios the depth of the transition zone at the Long Shot working point is between 740 and 790 m to the top of the zone and between 1,520 and 1,560 m to the bottom of the transition zone. The depth of the Long Shot working point is 701 m. The resulting transport time for ground water flowing from the working point to the sea floor ranges from approximately 400 years to 1,400 years when the sills are accounted for in the model. If the sills are not included in the model the travel time for the likely scenarios ranges from 1,400 years to 4,700 years. The range of travel time determined in this modeling effort is within the range of travel times obtained in the DRI study (2002). However, it should be noted that the values of porosity used by DRI ranged from as low as  $1.024 \times 10^{-5}$  to a maximum of  $5.2 \times 10^{-3}$ , while the porosity used in this study was 0.10 as determined in the MT study at the depth of the Long Shot working point. Lower values of porosity correspond to shorter travel times due to the increase in seepage velocity. Wheatcraft (1995) calculated a travel time of 880 years. The porosity used by Wheatcraft to calculate this travel time is unknown. Future modeling efforts include adding the third dimension, which will include the faults on both sides of the Long Shot working point, adding additional subsurface features shown in the MT results, and adding the cavity and chimney to the model.

# 1. INTRODUCTION

The objective of this study is to characterize the ground-water flow through the basin in which the Long Shot test was conducted. To meet this objective a two-dimensional ground water flow model of a cross section through the Long Shot site was developed. This model incorporated values from literature data and magnetotelluric (MT) data taken summer 2004. Several homogeneous and layered scenarios were modeled in order to calibrate the modeled data to the MT data. Results from this study will provide additional insight into the location of the sea floor discharge zones and ground-water flux rates, which will enable a better prediction of radionuclide transport rates.

## 1.1. Geology

From 1964 to 1972, prior to the underground detonations, U.S. Geological Survey (USGS) performed extensive studies on the geology and hydrology of Amchitka Island. Merritt and Fuller (1977) summarize the geologic history of Amchitka Island. Amchitka Island is a part of the Aleutian Island arc consisting of a curving submarine trench as deep as 7,600 m (Merritt and Fuller, 1977). The arc extends from the Gulf of Alaska across the north Pacific to Kamchatka with a parallel ridge rising to the north. The western part of this ridge is the Aleutian Islands and the eastern part is the mountainous Alaska Peninsula. A zone of convergence exists along the Aleutian arc although, most of the tectonic features are of probable tensional origin. Faulting, differential uplift, marine, stream, and glacial erosion predominant along the Aleutians have disturbed Amchitka Island (U.S. Army Corps of Engineers and USGS, 1965).

The island has a strongly developed joint and fault system. Submarine topography of the north side of the island displays southeast-trending linear scarps, ridges and troughs paralleling the island whereas the south side of the island shows northeast-trending scarps, ridges, troughs that lie normal to the trend of the island. The faulting and jointing of the island may be reflected by these northeast-trends. Although this area of the Aleutian Chain is one of the most active earthquake belts in the world, earthquake epicenters occur mainly south of the Chain and west of Adak (Perry and Nichols, 1965).

The bedrock of Amchitka Island is primarily Tertiary submarine and subaerially deposited volcanoclastic rocks with subordinate lava flows and intrusive units (U.S. Corps of Engineers and USGS, 1965). Carr and Quinlivan (1969) reported four major stratigraphic formations on Amchitka: older breccias and hornfels, the pillow lavas and breccias of Kirolof Point, the Banjo Point Formation, and the Chitka Point Formation. The eastern part of the island is divided into two main units; the Chitka Point Formation and the overlying Banjo Point Formation. The Chitka Point Formation is estimated to be in excess of 4,900 m (Gard and Hale, 1964). At the central and western part of the island the Chitka Point consists of sandstone, conglomerate, and volcanic breccia. The formation of the southeastern half of the island is the Banjo Point formation of Oligocene or Miocene age. It is estimated to be more than 3,000 m thick and

mainly composed of volcanic breccia. The porosity of the Banjo Point Formation ranges between 4 and 26 percent (Gard and Hale, 1964).

### **1.1.1. Geology of the Long Shot site**

The Long Shot site is underlaid by 1,220 m of Banjo Point formation (Gard and Hale, 1964). Tertiary volcanic tuffs and breccias are bounded by fractures and/or fault zones on the northwest, southeast, and southwest sides (U.S. Army Corps of Engineers and USGS, 1965). At ground zero, the rocks are altered pyroclastic rocks of andesitic and basaltic composition. The trend of the lineations is generally transverse to the island (N 55°E to N 60°E) near the Long Shot site (Gard and Hale, 1964).

Starting 1964, the U.S. Corps of Engineers did exploratory drilling for the Long Shot detonation. Vertical and directional holes EH-1, EH-3, EH-5, EH-5a, EH-6, and EH6-a were successfully cored and logged (U.S. Army Corps of Engineers and USGS, 1965). The core logs can be seen in Figures B-1 – B-3. In addition, geophysical and directional surveys were made. The emplacement hole for the Long Shot detonation, EH-5, was drilled vertically to a depth of 750 meter below sea level (mbsl). At 183 m northwest and southwest from EH-5, holes EH-3 and EH-6 were directionally drilled to cross hole EH-5 at 640 mbsl. Hole EH-1 was located 335 m north of EH-5 and close to a possible fault. This hole was drilled to a depth of 490 mbsl. Circulation of drilling fluid in this hole was lost in a series of open fractures and the hole was eventually abandoned.

The cores obtained from the exploratory drilling and from outcrop rocks are of volcanic material with a composition of basaltic andesite or andesitic basalt (U.S. Corps of Engineers and USGS, 1965). Breccias and tuffs are the primary rock types. Pyroclastic and intrusive rocks are less representative. The core holes consist of volcanic material of Banjo Point Formation ejected, intruded, or extruded from the Oligocene or Miocene time. The breccias occur in units of few meters to few hundred meter thickness. Common fragment sizes of the breccias are 13 to 152 mm (rare maximum dimension of few meters). Only a small percentage of the total stratigraphic section consists of tuff. The tuffs have angular to subangular fragment sizes of maximum 13 mm that consists of pumice and ash. Finer clastics in units of few meters to several meters thickness can be seen between the breccia units with grain sizes ranging from silty clay shale to coarse volcanic sandstone. The volcanic sandstone and siltstone are mixed with subangular and subrounded grains. Sizes range from 6 mm to silt size. Andesite sills encountered between a depth of 679 and 771 mbsl, include 90 percent crystalline andesite. A large portion of the crystalline andesite is 1.6 mm laths of feldspar. Ferro-magnesian minerals of sizes 1.6 to 3.2 mm are also common.

One notable stratigraphic feature in this region of the island is the two layers of andesite encountered in EH-3, EH-5, EH-5a, and EH6a between depths of 679 and 771 mbsl. The “main andesite” is about 76 m thick overlaid by a 4.6 m thick layer, referred to as the “first andesite”. A layer of tuff and siltstone is embedded in between the andesite sills.

The U.S. Army Corps of Engineers and USGS (1965) provided a general correlation of the core logs between holes EH-3, EH-5, and EH-6 (U.S. Army Corps of Engineers and USGS, 1965). In EH-5, at 489 mbsl, a possible marker horizon of welded tuff is encountered and can be compared to a thin bed found at a compatible depth in EH-3 and EH-6. Clear-cut correlations can be made near the intersection point of the core holes and where the borings are within 30 m or less of each other. When looking at overlying gross units, general correlations can be made but there is no certainty where top or bottom of such a unit is located. The andesite encountered in holes EH-3 and EH-5 nearly corresponds to andesite found in the quarry at Hill 165 located 2.7 km northwest of Long Shot. There are both similarities and dissimilarities in petrographical and chemical studies between the andesite in EH-5 and the quarry outcrop, however a correlation between the locations cannot be proved or disproved. The andesite at the quarry dips 12° to 16° southeast. A dip of 14° would carry the andesite to the same depth as the main andesite at EH-5. Sea-cliff strata in this area show a southeast dip of 5° to 15°. A lithologic correlation can be made between core holes EH-3, EH-5, and EH-6 but not with core hole EH-1 (U.S. Army Corps of Engineers and USGS, 1965).

## **1.2. Hydrology**

A long-term hydrologic network was established on Amchitka Island in 1967 and continued through August 1974. The hydrologic studies were prompted by the potential of using Amchitka Island as a location for high yield testing. Surface water gaging stations and ground-water observation wells were installed at potential sites for possible high yield emplacement holes. Ground-water investigations performed during this investigation included water level monitoring in test wells and other holes. Furthermore it included a detailed testing of deep exploratory holes at actual and potential test sites across the island. The investigation also integrated surface study of hydrologic features such as springs, terrestrial seeps, and perennial lakes and streams.

Because of the Island's remoteness, little data was collected before and after the long-term hydrologic network in the late 60's. Reported mean annual precipitation for February 1943 through June 1948, and from October 1967 through June 1972 was 828 and 953 mm respectively. Gard and Hale (1964) computed a recharge rate to range between 4 and 12 percent of 889 mm annual precipitation. This rate was based on flow net model, head distribution, and estimated hydraulic conductivity for Long Shot.

The lower plateaus of Amchitka Island are composed of small drainage basins and hundreds of small lakes and ponds (Gonzalez, 1977) with bottoms of low permeability materials (Merritt and Fuller, 1977). Precipitation temporarily stored in the lakes and mantle of tundra and peat moves directly to the stream channels or laterally to the stream courses and thereafter discharge into the ocean (U.S. Army Corps of Engineers and USGS, 1965). The upper few meters to a few hundred meters beneath the surface of Amchitka Island consist of permeable materials such as tundra, soil, peat, and fractured and weathered volcanic rocks (Merritt and Fuller, 1977). At shallow observation wells a rapid

response in water levels could be seen during precipitation events. This response indicates a high infiltration rate in the top few meters of the subsurface. Moreover, a clay zone is present at the base of the tundra and peat in some areas across the island, which retards the recharge to the bedrock (U.S. Army Corps of Engineers and USGS, 1965). These two observations lead to the conclusion that a large fraction of precipitation infiltrates and flows through shallow aquifers and discharges to surface bodies. Gonzalez (1977) and Merritt and Fuller (1977) performed a comparison between precipitation and runoff altitude relationships and concluded that most precipitation results in surface water runoff. At several test holes the water level was within few meters of the land surface which implies that the sediment of the lowland parts of the island is saturated essentially to land surface. Gonzalez (1977) and Merritt and Fuller (1977) also suggest that the water table is at or very near surface over most of Amchitka Island.

According to hydraulic tests and temperature surveys, the hydraulic head decreases with depths and the overall direction of ground-water flow beneath most of Amchitka is downward (Gonzalez, 1977). The ground water is most likely flowing from approximately the central part of the island towards the coast as is constant with island ground-water hydrology (U.S. Army Corps of Engineers and USGS, 1965). This ground-water flow pattern could be changed by the inclined bedding of the sediments and intrusive rocks, which would result in a diversion of the flow to the coast within a few kilometers of a recharge area by the numerous cross-cutting, permeable, and near vertical fracture zones. In addition, hydraulic testing has also shown that primary avenues for fluid movement are fractures such as joints and faults. Fracture intensity decreases with depth due to a tendency of fracture closing under greater lithostatic loads (Gonzalez, 1977 and Merritt and Fuller, 1977). These features decrease the transmissivity with depth (Merritt and Fuller, 1977). The zeolite and chlorite in fractures and cavities of the older (deeper) breccia also reduce the effective porosity and permeability (Merritt and Fuller, 1977).

U.S. Army Corps of Engineers and USGS (1965) reported a moderate permeability of the near-surface materials. Recharge is significantly less than the surface runoff implying an average permeability of the upper rock units to less than  $4.72 \times 10^{-7}$  m/s (U.S. Army Corps of Engineers and USGS, 1965). Hydrologic and geologic tests imply that the water-bearing zones of the bedrock units underlying the surface at shallow depths is up to three orders of magnitude less permeable than  $4.72 \times 10^{-6}$  m/s (U.S. Army Corps of Engineers and USGS, 1965).

### **1.2.1. Hydrology of the Long Shot site**

Long Shot was detonated at a depth of 701 m below land surface (mbls) and within the Banjo Point Formation. The site is divided by linear features (faults or lineations) that express probable near-vertical permeable fracture zones (U.S. Army Corps of Engineers and USGS, 1965). Two northeast-trending linear features are located at 610 m apart on each side of the Long Shot site. Hazleton-Nuclear Science Corporation (1964) estimated a hydraulic conductivity of these features to be  $3.53 \times 10^{-4}$  m/s. Furthermore, a north-trending feature cuts

the two northeast-trending features about 2,410 m from the coast (U.S. Army Corps of Engineers and USGS, 1965).

Both the Banjo Point formation and the andesitic sill have very little interstitial permeability (U.S. Army Corps of Engineers and USGS, 1965). The andesite sills encountered between 679 to 771 mbsl contain cooling joints and tectonic features. When comparing with the bulk of the bedrock, the sills are of moderate hydraulic conductivity and, thus affect the overall ground-water flow. The hydraulic conductivity of the fractured sill units is from  $4.72 \times 10^{-8}$  to  $4.72 \times 10^{-7}$  m/s, which is slightly greater than the hydraulic conductivity of the Banjo Point bedrock. A bulk hydraulic conductivity of the Banjo Point formation is approximately  $3.53 \times 10^{-8}$  m/s (Hazleton-Nuclear Science Corporation, 1964). However, the Banjo Point formation possibly has an overall greater hydraulic conductivity than indicated from the swab and pump tests (U.S. Army Corps of Engineers and USGS, 1965). As noted in the report published by the U.S. Army Corps of Engineers and USGS (1965), drilling practices could have altered the hydraulic conductivity in a radial area surrounding each observation well. Water level fluctuations in observation well EH-1 when EH-3, -5, and -6 were being drilled provided evidence of a relatively higher hydraulic conductivity in the formation suggesting, but not confirming, a hydraulic connection between permeable fractures in the Banjo Point formation. Opposing this suggestion is the fact that no drawdown responses could be seen in nearby mud filled holes when swabbing and pumping tests were performed in EH-5. The explanation could be that conditioned drilling fluids were used to reduce circulation losses and existing mud-filled fractures were not reopened. This would affect results from the swabbing and pump tests and consequently, hydraulic conductivities of the aquifer would have been underestimated. A higher permeability of the formation than reported was also indicated by increased water losses out of the bore hole as well as a greater number of reported fractures were reported in EH-3, which was directionally drilled across the principal fracture grain. In summary, the most permeable of the Banjo Point formation is the fracture zones followed by a moderate permeability in the sills and the bulk of the formation is poorly permeable. Considering the thickness of the sills in comparison to the fractured zones, the sills are more transmissive and, thus constitute the major pathway for ground-water flow. The principal recharge to the system at the Long Shot site is most likely along the fracture zones.

Hole EH-1 was drilled to a depth of 490 mbsl and close to or on the northeast-trending fault located north of Long Shot (U.S. Corps of Engineers and USGS, 1965). Numerous open fractures were found during drilling and the permeability of this zone is about  $4.72 \times 10^{-7}$  to  $4.72 \times 10^{-6}$  m/s with an estimated effective porosity of 1 %. As mentioned above, the hydraulic conductivity of this fault is estimated to  $3.53 \times 10^{-4}$  m/s. In hole EH-5, the hydraulic conductivity of the fractured andesite sill units is between  $4.72 \cdot 10^{-8}$  to  $4.72 \cdot 10^{-7}$  m/s with an estimated effective porosity of 0.1 %. The permeability of the Banjo Point formation above the sills is approximately  $4.72 \times 10^{-9}$  m/s with an estimated effective porosity of 0.01 %. This permeability can also, as explained above, be somewhat higher. Based on swab tests in hole EH-5 and pumping tests in EH-1



and EH-5, Gard and Hale (1964) estimated an overall hydraulic conductivity of the aquifer system ranging between  $1.04 \times 10^{-7}$  and  $3.53 \times 10^{-7}$  m/s.

The general ground-water flow pattern is from the central part of the island towards the coast. Many features such as fractures and inclined bedding of sediments will influence this pattern. The fractured andesite sill units with higher hydraulic conductivity compared to the average hydraulic conductivity of the Banjo Point formation is an important feature that needs to be taken into consideration when looking at the ground-water flow pattern. The U.S. Army Corps of Engineers and USGS (1965) suggest three different cases of ground-water circulation at the Long Shot site.

Case 1 assumes that the andesite sill is the only water transporting unit and that the andesite unit is continuous with the andesite that was encountered at the quarry 2.7 km north of EH-5. The circulation pattern would be northward to the sea from the outcrop area towards EH-5. More permeable fracture zones and vertical faults intercepting the andesite sills are not taken into account which makes this pattern unlikely.

Case 2 assumes that no ground water flows in the bedrock block between the fracture zones and that that no recharge occurs to the bedrock. The andesite sill is assumed continuous. Water should then move from the fracture zones into the sills at the Long Shot site. Movement of water near shore and seaward will occur from the sills to the fracture zones and discharge in the ocean.

Case 3 assumes permeability of the bedrock block above and below the sills and between the fracture zones approximately the same as the sills. This would result in a somewhat less travel time for the water to move from EH-5 to the ocean compared to case 2. Also, a larger volume of water would discharge to the ocean.

In this study, a two dimensional combination of case 2 and 3 was investigated. It was assumed that the andesite sill unit is continuous. The permeability of the bedrock block above and below the andesite sills and between the fracture zones is smaller than the sill. Recharge occurs to the bedrock and ground water flows in the fractured bedrock.

### **1.3. Freshwater saltwater interface**

Beneath oceanic islands, a lens of freshwater sits above relatively denser saltwater. In the ideal case of a homogeneous and isotropic island, the freshwater body assumes a lenticular shape bounded at its base by a concave-upward surface. The infiltrating water flows laterally and thereafter upward exiting in seepage zones along the shoreline. The freshwater lens is therefore greatest under the central part of the island. In the central part of the island close to the Long Shot site, U.S. Army Corps of Engineers and USGS (1965) estimated the interface between freshwater and saltwater at greater than 760 mbsl. Several methods have been formulated to estimate the freshwater interface with saltwater in coastal and island aquifers. Each of these methods as they apply to the island will be briefly discussed.

### *Ghyben-Herzberg relationship*

Assuming the fresh water and saltwater to be immiscible and the liquids are hydrostatic, the freshwater-saltwater interface can be found by using the Ghyben-Herzberg relationship (Fenske, 1972). This relationship results in an interface between the freshwater and saltwater at a depth of 40 times the elevation of the water table above sea level. Considering the ground surface elevation at the Long Shot site to be 43 m (U.S. Corps of Engineers and USGS, 1965) an interface depth of 1707 mbsl at the working point of Long Shot is calculated. However, in actuality a sharp interface between the two fluids does not exist instead a mixing or dispersion zone through the action of ocean tides, seasonal fluctuations of the water table, diffusion in response to salinity, density gradient of saltwater, and temperature gradients. The assumption of hydrostatic fluids eliminates discharge of the fresh water, instead the actual lens extends out under the sea floor and provides a discharge area for the fresh ground water. In addition, there is also a head loss due to friction from the fresh ground water that seeps through the rocks. The assumptions that make up this relationship results in an overestimation of the interface between the freshwater and saltwater.

### *Potential Method*

The potential method can also be used in order to locate the freshwater saltwater interface (Fenske, 1972). By using piezometer wells at different depths throughout the system, the potential distributions in the lens can be found. From potential data at EH-1 and EH-5 Fenske (1972) estimated the bottom of the fresh water lens to 1,120 mbsl at the working point of Long Shot.

### *Water Analysis Method*

Water samples taken at various depths give a total dissolved-solids distribution from which the interface can be obtained. In EH-5, the water contained between 300 and 500 ppm chloride at a depth of 671 to 792 mbsl (Fenske, 1972). This result implies a freshwater saltwater interface close to this depth.

### *Magnetotelluric*

In summer 2004, magnetotelluric measurements were performed in order to locate the freshwater saltwater interface depth (Unsworth et al., 2005). It was concluded that increasing salinity is between 700 and 1,500 m at the Long Shot site. Furthermore, Unsworth et al. (2005) state that the depth of the fresh to saltwater interface is approximately at 1,600 m. Due to non-uniqueness of the data analysis the depth could also be in the range 1,400 to 2,100 m. The transition zone (TZ) used in the ground water modeling performed in this report was thus chosen to range between 700 and 1,600 m.

## **1.4. Previous ground water models of Long Shot**

Several ground-water models of the Long Shot site have been developed by others. Wheatcraft (1995) modeled the ground water system of Amchitka Island with the finite element program SUTRA. The island was assumed as isotropic and homogenous system. Furthermore, the recharge was assumed to be

spatially and temporally constant from the island surface. It was concluded that, the dimensionless recharge/hydraulic conductivity ratio is  $6.88 \cdot 10^{-3}$  in order for a freshwater saltwater interface 1,200 m to be modeled. Wheatcraft (1995) used a recharge of 0.1 m/year which resulted in a hydraulic conductivity of the rock matrix as  $4.63 \cdot 10^{-7}$  m/s. He estimated the longitudinal dispersivities to 33.3, 66.7 and 133 m and transverse dispersivity was chosen as a tenth of the longitudinal dispersivity.

Hassan et al. (2002) modeled ground-water flow and transport of radionuclides at Amchitka. The finite element program "Finite Element Subsurface Flow system" (FEFLOW) was used and this model is referred to as the Desert Research Institute (DRI) model. The island was modeled as homogenous, anisotropic, and no spatial variability except at the cavity and chimney. Head and concentration data were used to find the hydraulic conductivity and recharge values. Different random values of hydraulic conductivities were selected in a Monte Carlo fashion. For Long Shot, their calibration resulted in a hydraulic conductivity of  $1.83 \cdot 10^{-7}$  m/s and a recharge of  $10^{-4}$  m/day. The recharge/hydraulic conductivity ratio was thus  $6.3 \cdot 10^{-3}$ . Estimated longitudinal and transverse dispersivities were 100 and 10 m respectively.

## **2. METHODOLOGY**

The Long Shot site ground-water flow pattern was modeled with the finite element program FEFLOW. FEFLOW is a three-dimensional density dependent, mass and heat transport model available from Water Resources Planning and Systems Research Ltd. (WASY). Several scenarios were modeled by using literature values for recharge and hydraulic conductivities. For example, choosing a reported hydraulic conductivity value for the rock matrix, values for recharge and longitudinal and transverse dispersivities were changed in the model until the location of the freshwater and saltwater dispersion zone corresponded to the MT results. For this modeling attempt, the Long Shot site was modeled in 2-D with a cross section perpendicular to the long axis of the island. This profile is the same as the profile along which the magnetotellurics data was collected and will be referred to as the Long Shot profile, (Unsworth et al., 2005). The model was built with bathymetry data from the Amchitka Expedition in 2004 (Johnson et al., 2005) and the topography data was obtained from Space Shuttle Radio Topography (SRTM, 2005). Currently, a three dimensional model of the Long Shot site is being built and results from these simulations will be published at a later date. Models will also be developed for Milrow and Cannikin sites.

### **2.1. Geometry and boundary conditions of the model**

Earlier conceptual models (Fenske, Wheatcraft, and DRI) assumed the ground-water divide in the middle of the island and, thus, only modeled half of the island. This current modeling attempt incorporates actual topography and the andesite sills necessitating modeling of the entire cross section from the North Pacific coast to the Bering Sea coast. Bathymetry data was obtained from the Amchitka

expedition, 2004 (Johnson et al., 2005). Topography data was obtained from the Space Shuttle Radio Topography (SRTM) (SRTM, 2005). In order for the freshwater lens not to be affected by the finite element model boundaries, a total cross section width of 16 km was used. The highest surface elevation at the Long Shot profile is 47 m above sea level and the lower boundary condition was at 3,000 mbsl.

The finite mesh was generated automatically in FEFLOW. Approximately 193,000 triangular elements were used for the homogeneous simulations. At about 500 to 1,000 mbsl, a finer mesh was generated in order to account for the andesite sill layer which resulted in a mesh with approximately 255,000 elements. Figure 2-1 shows the mesh geometry and boundary conditions of the model. A constant flux (recharge) was used for the boundary on the island (red). The ocean was modeled as a hydrostatic pressure boundary condition (blue). A no-flow boundary was specified for the bottom of the model. Lateral boundaries were established at a sufficient distance from the subsea discharge zones resulting in a cross section width of 16 km. The green line illustrates the location of the emplacement hole of Long Shot.

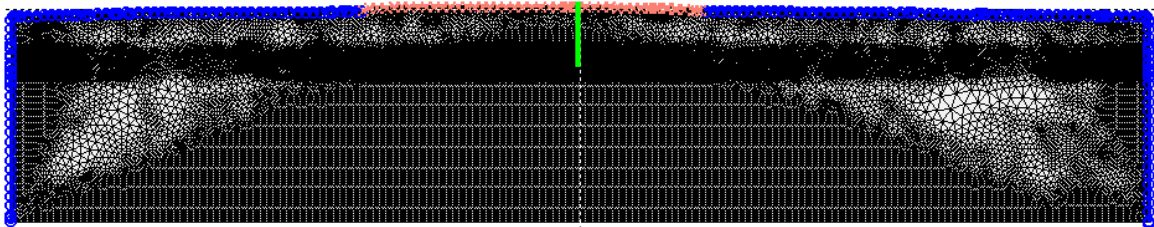


**Figure 2-1** Mesh geometry and boundary conditions. Green line shows location of the emplacement hole of Long Shot. Red is the recharge and blue is the hydrostatic pressure. The bottom boundary is modeled as a no-flow boundary.

## 2.2. Base-case parameters

Mark et al. (2005) reported an average seawater concentration of approximate 33,000 mg/l. In all simulations a seawater concentration of 33,000 mg/l was used. Freshwater and saltwater densities were 1,000 and 1,026 kg/m<sup>3</sup> respectively. Unsworth et al. (2005) indicated a porosity of 0.1 at the depth of the Long Shot working point. Thus the porosity was set to 0.1 in these simulations.

## 2.3. Calibration of the model

In order to calibrate the model, parameters such as recharge, hydraulic conductivity, and transverse and longitudinal dispersivities were varied. The model was calibrated to the top and bottom of the dispersion zone determined by magnetotelluric measurements in 2004 (Martyn et al., 2005). According to the MT data the saltwater occur at 1,600 mbsl at the Long Shot site. The transition zone is approximately 900 m and located approximately between 700 and 1,600 m. The first simulations assumed the island to be homogeneous (no sills). To address the heterogeneity of the island, the andesites sills were added to the model in additional simulations.

### 2.3.1. Scenarios investigated

#### *Homogeneous scenarios*

A homogeneous subsurface were used in six scenarios. Two scenarios used literature values for the recharge and four scenarios used literature values for the hydraulic conductivity of the rock matrix. For the first scenario a literature value of recharge was used. The hydraulic conductivity of the subsurface was thereafter changed until a freshwater saltwater transition zone was located at 700 to 1,600 m and matching the MT results. Once the first scenario was calibrated a recharge/hydraulic conductivity ratio,  $N_{rk}$ , was calculated to aid in finding the hydraulic conductivity or the recharge for the other scenarios. For the scenarios where a literature value for recharge was used, the hydraulic conductivity was found by dividing the recharge with  $N_{rk}$ . Similarly, for the scenarios where reported values for hydraulic conductivities were used, the recharge was calculated by multiplying the hydraulic conductivity with  $N_{rk}$ .

#### *Andesite sill layer scenarios*

At the Long Shot site, the andesite sill layer was recognized by the U.S. Army Corps of Engineers and USGS (1965) as an important feature for ground water flow. The depth of this layer is between 678 and 771 mbsl (U.S. Army Corps of Engineers and USGS, 1965). The lateral extent and width of this layer are not known. Thus, both the width of the andesite sill layer and the lateral location were changed until the shape and location of the transition zone matched the MT results. Due to time constraints two scenarios with a layer representing the andesite sills were modeled. This layer had a higher hydraulic conductivity compared to the rock matrix. These two scenarios used literature values of recharge and the hydraulic conductivity of the rock matrix and the andesite sill layer as well as the extent of the layer was changed to match the MT results.

### 2.3.2. Recharge and hydraulic conductivity

In the model, recharge estimation from Gard and Hale (1964) was used and calculated from average annual precipitation in Merritt and Fuller (1977). Hydraulic conductivities for the Banjo Point formation, the fractured andesite sill units, and the units above the andesite sill were obtained from U.S. Army Corps of Engineers and USGS (1965) and used in the modeling. In addition, hydraulic conductivities of the aquifer at Long Shot site reported by Gard and Hale (1964) were also used in the simulations. Reported values can be seen in Table 2-1. The calibration process consisted of selecting a reported value for one of the parameters (either recharge or hydraulic conductivity) and changing the other parameter until a dispersion zone ranging between 700 and 1,600 mbsl which correspond to the MT results was found. In order fit the skewness of the MT results, the hydraulic conductivity of the andesite layer was chosen as one or two orders of magnitude greater than the rock matrix.

**Table 2-1** Recharge, precipitation, hydraulic conductivities (K) values as reported by Gard and Hale<sup>(1)</sup> (1964), U.S. Army Corps of Engineer and USGS<sup>(2)</sup> (1965), and Merritt and Fuller<sup>(3)</sup> (1977).

<b>Recharge</b>	
Min <sup>(3)</sup> , $R_{min}$ , (m/day)	$9.07 \cdot 10^{-5}$
Max <sup>(3)</sup> , $R_{max}$ , (m/day)	$3.13 \cdot 10^{-4}$
<b>Hydraulic conductivity</b>	
Banjo Point formation <sup>(2)</sup> , $K_{Banjo}$ , (m/s)	$3.53 \cdot 10^{-8}$
Above andesite sills <sup>(2)</sup> , $K_{Abovesill}$ , (m/s)	$4.72 \cdot 10^{-9}$
Fractured andesite sill units <sup>(2)</sup> , $K_{sills}$ , (m/s)	$4.72 \cdot 10^{-8}$ to $4.72 \cdot 10^{-7}$
Long Shot aquifer <sup>(1)</sup> , $K_{LS}^{min}$ , (m/s)	$1.06 \cdot 10^{-7}$
Long Shot aquifer <sup>(1)</sup> , $K_{LS}^{max}$ , (m/s)	$3.53 \cdot 10^{-7}$

### 2.3.3. Transverse and longitudinal dispersivities

Transverse and longitudinal dispersivities have not been determined for Amchitka Island. In a different aquifer (other than Amchitka) Gelhar et al (1982) reported a longitudinal/transverse ratio of 0.6 for brecciated basalt interflow zone. Again at a different aquifer, a longitudinal/transverse ratio for basaltic lava and sediments was documented by Robertson, (1974) as 910/1370. Wheatcraft (1995) used a longitudinal dispersivity from 133 to 33.3 m the transverse dispersivity was a tenth of the longitudinal dispersivity for the ground-water model developed for the Long Shot site. DRI (2002) used a longitudinal and transverse dispersivity for the Long Shot site of 100 and 10 m respectively. In the simulations presented in this report, longitudinal and transverse dispersivities ( $\alpha_L$  and  $\alpha_T$ ) were altered until a freshwater saltwater transition zone of 900 m was reached which matched the MT results.

## 3. RESULTS

Several scenarios were modeled by using literature values for recharge and hydraulic conductivities. Recharge was calculated by using Gard and Hale's (1964) estimation of 4 to 12 % of the precipitation. Hydraulic conductivities values were reported from U.S. Army Corps of Engineers and USGS (1965) and Gard and Hale (1964). These values are listed in Table 2-1.

### 3.1. Calibration to magnetotelluric data

#### 3.1.1. Homogeneous

Calibration of the model to the MT results with a transition zone at 700 to 1,600 mbsl at the Long Shot working point considering homogeneity in hydraulic conductivity was done by changing hydraulic conductivity and recharge within reported or reasonable ranges. For a dispersion thickness of 900 m to be modeled, the longitudinal and transverse dispersivities were also changed. Longitudinal and transverse dispersivities were adjusted to calibrate the model to the transition zone measured by MT.

### Scenario 1 ( $R_{min}$ )

The calculated minimum recharge of  $9.07 \times 10^{-5}$  m/day was kept constant in this scenario and hydraulic conductivity was varied to obtain a match to the MT results. To fit the MT results, several simulations resulted in a hydraulic conductivity of  $2.3 \times 10^{-7}$  m/s which is in the same order of magnitude as the hydraulic conductivity ( $3.5 \times 10^{-7}$  m/s) estimated for the Long Shot site by Gard and Hale (1964). Also, the longitudinal and transverse dispersivities were 90 and 10 m respectively. These values resulted in a transition zone between 680 to 1,560 mbsl. On the east side of the island, the freshwater discharges up to 20 m off the shore-line. The transition zone ends (where the salinity of the water approaches the salinity of seawater) approximately 1,360 m from shore. The ground water travel time from the working point of Long Shot to the marine environment is approximately 4,700 years. It should be noted that this travel time changes with porosity. The fracture porosity is not known on Amchitka Island. In these simulations a porosity of 0.1 was used according to porosity the travel time will decrease. Results can be seen in Table 3-1. Figure 3-1 shows the resulting freshwater lens and transition zone of the Long Shot site. Red color illustrates saltwater with a concentration of 33,000 mg/l and blue illustrates freshwater. A full description of the color code is provided in Appendix A. Furthermore, the 200 and 32,800 mg/l isolines and the pathline from the working point of Long Shot are illustrated in Figure A-2 in Appendix A. The minimum recharge scenario resulted in a recharge/hydraulic conductivity ratio of  $4.56 \times 10^{-3}$ . This ratio was used in the homogeneous simulations to find approximate values of the recharge or hydraulic conductivity in order to model a transition zone from 700 to 1,600 mbsl.

### Scenario 2 ( $R_{max}$ )

For the maximum recharge scenario a calculated maximum recharge of  $3.13 \times 10^{-4}$  m/day was kept constant while varying hydraulic conductivity of the rock matrix. A hydraulic conductivity of  $7.9 \times 10^{-7}$  m/s was calculated from the recharge/hydraulic conductivity ratio of  $4.56 \times 10^{-3}$ . This hydraulic conductivity is in the same order of magnitude as estimated by Gard and Hale (1964) for the aquifer at Long Shot site and resulted in a transition zone from 680 to 1,560 mbsl. Figure A-3 illustrates the isolines and pathline from the working point of Long Shot. Longitudinal and transverse dispersivities of 120 and 10 m respectively were used (see Table 3-1). On the east side of the island, the freshwater discharges 20 m off shore. The transition zone ends approximately 1,360 m from the shore line on the Bering Sea side of the island. Ground water travel time from the working point of Long Shot is approximately 1,400 years.

**Table 3-1** Simulation results from the homogeneous scenarios where measured values of recharge was given. Hydraulic conductivities (K), longitudinal and transverse dispersivities ( $\alpha_L$  and  $\alpha_T$ ) were changed until the location of the transition zone (TZ) was approximately between 700 to 1,600 mbsl.

K (m/s)	$\alpha_L$ (m)	$\alpha_T$ (m)	TZ (mbsl)	Start of TZ distance from off- shore	End of TZ from off- shore (m)	Travel time from LS to sea level (years)
------------	-------------------	-------------------	--------------	---	--	---

	(m)						
<b>Scenario 1</b> <i>(R<sub>min</sub>)</i>	$2.3 \times 10^{-7}$	120	10	680 – 1,560	20	1,360	4,700
<b>Scenario 2</b> <i>(R<sub>max</sub>)</i>	$7.9 \times 10^{-7}$	120	10	680 – 1,560	20	1,360	1,400

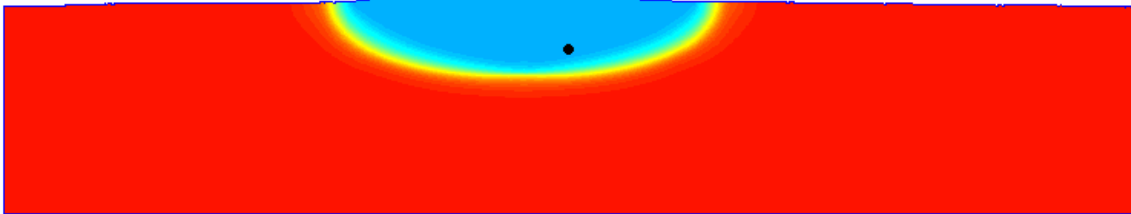


**Figure 3-1** Freshwater saltwater cross section for a homogeneous model. Black circle shows the working point of Long Shot. Red illustrates a saltwater content of 33,000 mg/l and blue illustrates freshwater. A full description of the color scale can be seen in Figure A-1.

### Scenario 3 ( $K_{Banjo}$ )

A homogeneous hydraulic conductivity of  $3.53 \times 10^{-8}$  m/s, which corresponds to the reported value for the Banjo Point Formation was used in this scenario. The recharge value for this scenario was calculated from the recharge/hydraulic conductivity ratio of  $4.56 \times 10^{-3}$ . The resulting value of  $1.4 \times 10^{-5}$  m/s is in the same order of magnitude as the minimum recharge calculated from precipitation and the minimum recharge estimation of 4 % by Gard and Hale (1964). Longitudinal and transverse dispersivities of 120 and 10 m respectively were assigned in order for a transition zone of 680 to 1,560 mbsl to be modeled. Isolines and pathline from the working point of Long Shot are illustrated in Figure A-4. On the east side of the island, the freshwater discharges 20 m off shore. The transition zone ends approximately 1,360 m from shore on the Bering Sea side of the island. The ground water travel time from the working point of Long Shot is 30,700 years. Table 3-2 lists results from simulations where reported values of hydraulic conductivities were used for the rock matrix.

### Scenario 4 ( $K_{Abovesill}$ )

In this scenario the reported hydraulic conductivity of the rock matrix above the sills ( $4.72 \times 10^{-9}$  m/s) was assigned as the homogenous hydraulic conductivity and recharge ( $1.9 \times 10^{-6}$  m/day) was obtained from the recharge/ hydraulic conductivity ratio. The recharge value is one order of magnitude less than the recharge calculated from the minimum precipitation and the 4 % recharge that was estimated by Gard and Hale (1964). This resulted in a transition zone between 680 and 1,560 m when a longitudinal and transverse dispersivity of 120 and 10 m respectively were used in the model. Figure A-5 shows the isolines and the pathline from the working point at Long Shot. Freshwater discharged 20 m off shore on the Bering side of the island. The transition zone ended approximately 1,360 m from shore on the east side of the island. Ground water travel time from the working point of Long Shot is in this scenario  $2.3 \times 10^5$  years.



*Scenarios 5 and 6 ( $K_{LS}^{min}$  and  $K_{LS}^{max}$ )*

The homogenous value of  $1.06 \times 10^{-7}$  m/s for hydraulic conductivity used in scenario 5 represents the minimum value in the range in hydraulic conductivity for the Long Shot aquifer reported by Gard and Hale (1964). The maximum value of this range,  $3.53 \times 10^{-7}$  m/s, was used as the homogeneous hydraulic conductivity in scenario 6. The resulting recharges values for scenarios 5 and 6 calculated from recharge/hydraulic conductivity ratio were  $4.2 \times 10^{-5}$  m/d and  $1.4 \times 10^{-4}$  m/d, respectively. These recharge values are in the same order of magnitude as the recharge calculated from the 4% recharge estimation by Gard and Hale (1964). Longitudinal and transverse dispersivity values of 120 m and 10 m were used in both scenarios. A transition zone ranging from 680 to 1560 mbsl was generated from the values used in scenario 5. The isolines and pathline for this scenario are shown in Figure A-6. In scenario 6, the resulting transition zone ranges from 680 to 1,560 mbsl. The isolines and pathline from the working point are illustrated in Figure A-7. On the east side of the island, the freshwater discharges 20 m off shore in both scenarios 5 and 6. The transition zone ends 1,360 from shore at the Bering Sea side in both scenarios 5 and 6. Ground water travel time for scenario 5 and 6 are 10,200 and 3,100 years respectively.

**Table 3-2** Simulation results from the homogeneous scenarios where reported values of hydraulic conductivity were given in the model. Recharge, longitudinal and transverse dispersivities were changed until the location of the transition zone (TZ) was approximately between 700 to 1,600 mbsl.

	R (m/day)	$\alpha_L$ (m)	$\alpha_T$ (m)	TZ (mbsl)	Start of TZ from off-shore (m)	End of TZ from off- shore (m)	Travel time from LS to sea level (years)
<b>Scenario 3</b> <i>(<math>K_{Banjo}</math>)</i>	$1.4 \times 10^{-5}$	120	10	680 – 1,560	20	1,360	30,700
<b>Scenario 4</b> <i>(<math>K_{Abovesill}</math>)</i>	$1.9 \times 10^{-6}$	120	10	680 – 1,560	20	1,360	$2.3 \times 10^5$
<b>Scenario 5</b> <i>(<math>K_{LS}^{min}</math>)</i>	$4.2 \times 10^{-5}$	120	10	680 – 1,560	20	1,360	10,200
<b>Scenario 6</b> <i>(<math>K_{LS}^{max}</math>)</i>	$1.4 \times 10^{-4}$	120	10	680 – 1,560	20	1,360	3,100

*Summary of homogeneous results*

Scenarios 1 and 2 both resulted in hydraulic conductivities in the same order of magnitude as compared to literature values. The hydraulic conductivity for scenario 1 falls within the range of literature values whereas the hydraulic conductivity of scenario 2 is slightly higher than reported values. If the assumption that the hydraulic conductivities at the Long Shot site are greater than the swabbing and pump test results indicate as discussed, then the results generated in both scenario 1 and scenario 2 are likely. The longitudinal dispersivities for these two scenarios are higher but in the same range as Wheatcraft (1995) and DRI (2002) used in their modeling efforts. Transverse

dispersivities are the same as Wheatcraft (1995) and DRI (2002) used. The thicker transition zone measured by MT can explain this result.

Scenarios 3 through 6 were modeled with literature values of hydraulic conductivity and the recharge value was changed in order for the location and thickness of the transition zone to correspond to the MT results. Scenarios 3, 5 and 6 resulted in recharge values in the same order of magnitude as reported literature values of recharge. For both scenarios 2 and 5, the recharge values were lower than reported values for recharge. Scenario 6 is within the same range as reported values. Scenario 4 resulted in a recharge value being one order of magnitude lower than calculated from the 4 % recharge estimation by Gard and Hale (1964).

To better compare resulting values of hydraulic conductivity and recharge for each scenario with measured values reported in literature, precipitation was calculated from recharge values using reported ranges of likely recharge to precipitation ratios. For example, if the modeled recharge is  $1.4 \times 10^{-5}$  m/day it would result in a daily precipitation of  $3.5 \times 10^{-4}$  m/day or 0.128 m/year for the 4 % recharge estimation. For scenario 3, the modeled recharge would result in an average yearly precipitation of 43 to 128 mm when using the 4 to 12 % recharge estimation by Gard and Hale (1964), which is much lower than measured values of 828 to 953 mm. These values would be even lower for the rock matrix above the sill scenario (scenario 4) because of the lower recharge that was used in the model. Given these results, scenarios 3 and 4 are not very probable.

Scenarios 5 and 6 modeled recharge values are in the same order of magnitude as the minimum recharge estimated by Gard and Hale (1964). Similar precipitation calculations as was made for scenarios 3 and 4 were performed. If the 4 to 12 % recharge estimation by Gard and Hale (1964) is used, the modeled recharge of the scenario 5 would result in a yearly precipitation range between 128 and 383 mm. Once again these values are lower than historically measured values causing questions about the validity of this scenario. For scenario 6 the yearly precipitation would range between 426 and 1288 mm when using the 4 to 12 % recharge estimation by Gard and Hale (1964). This scenario is thus a very likely scenario because it compares to the measured precipitation values. The comparisons of each parameter to literature values are summarized in Table 3-3. From this comparison it appears that scenario 1, 2 or 6 are most likely a reasonable model of ground water flow through the Long Shot site. This conclusion is further validated when one compares the magnitude of measurement error in hydraulic conductivity to precipitation. Point measurements of hydraulic conductivity were basically obtained in bore holes at the Long Shot site. Considering the highly heterogeneous nature of fractured rock and the error associated with the measurement one can discern that reported values may be off by as much as an order of magnitude. This is not to say that precipitation measurements do not have error associated with them, especially in locations with high wind speeds such as Amchitka. In general, for hydraulic conductivity measurements to be off by one order of magnitude is more likely than for precipitation measurements to be off by an order of magnitude.

The distance on the east side of the island where the transition zone ends is approximately 1,360 m. All scenarios model the freshwater discharge to 20 m off shore on the east side of the island.

The ground water travel time ranges from 1,400 to  $2.3 \times 10^5$  years with the longest travel time for the above the sill scenario (scenario 4) and shortest for the maximum recharge scenario (scenario 2).

**Table 3-3** Summary of modeled results for the homogeneous scenarios and how they fit to literature values.

	Constant parameter	Modeled parameter	In what order of magnitude modeled values compare to literature values	Likeness of scenario
<b>Scenario 1</b> ( $R_{min}$ )	Recharge	Hydraulic conductivity	Same order of magnitude	Likely scenario
<b>Scenario 2</b> ( $R_{max}$ )	Recharge	Hydraulic conductivity	Same order of magnitude	Likely scenario
<b>Scenario 3</b> ( $K_{Banjo}$ )	Hydraulic conductivity	Recharge	Same order of magnitude	Unlikely scenario
<b>Scenario 4</b> ( $K_{Abovesill}$ )	Hydraulic conductivity	Recharge	One order of magnitude too low	Unlikely scenario
<b>Scenario 5</b> ( $K_{LS}^{min}$ )	Hydraulic conductivity	Recharge	Same order of magnitude	Unlikely scenario
<b>Scenario 6</b> ( $K_{LS}^{max}$ )	Hydraulic conductivity	Recharge	Same order of magnitude	Likely scenario

### 3.1.2. Andesite sills influence on the ground water flow

The limited number of core logs at the Long Shot site provides little information about the subsurface. However, one prominent stratigraphic difference is the two andesite sill layers encountered in EH-5 at a depth 678 to 771 mbsl (U.S. Army Corps of Engineers and USGS, 1965). This layer was recognized by the U.S. Army Corps of Engineers and USGS (1965) as an important feature that influences the ground-water flow due to moderate hydraulic conductivity when compared to the main units at Long Shot site. Because a hydraulic conductivity was only given for these sills as a whole, one layer of sill from 678 to 771 mbsl was modeled. From the core logs, it is not possible to distinguish its lateral extent. The width of this layer was therefore varied in the cross section so that the depth and shape of the modeled transition zone would fit the magnetotelluric measurements. According to U.S. Army Corps of Engineers and USGS (1965), the hydraulic conductivity of the andesite sills were one to two orders of

magnitude greater than the rock formation. In the modeled scenarios where reported values of recharge were used and hydraulic conductivities of the rock matrix and the andesite sill layer were modeled, the hydraulic conductivity of the andesite sill layer was chosen as two orders of magnitude greater than the hydraulic conductivity of the rock matrix. Only scenarios with a two orders of magnitude difference between the andesite sill layer and the rock matrix were chosen due to time constraint. In order to duplicate the top of the transition zone as MT results show, several simulations resulted in a best fit to the magnetotelluric data with the location of the andesite layer at 1,000 m and 1,000 m west and east of Long Shot respectively. The thickness of the layer was from 679 to 771 mbsl. This positioning does not suggest that this location of the sill is the only location, but because of time constraints, this was the only location used in these simulations. From the homogeneous simulations the most likely scenarios were 1, 2, and 6 ( $R_{\min}$ ,  $R_{\max}$ , and  $K_{LS}^{\max}$ ). Two scenarios were chosen to be modeled with an andesite sill layer. One scenario was with the minimum recharge value and the other scenario was with the maximum recharge value as constant while changing the hydraulic conductivity of the andesite sill layer and the rock matrix in order to match the MT results.

#### *Scenario 7 ( $R_{sill}^{\min}$ )*

The calculated minimum recharge ( $9.07 \times 10^{-5}$  m/day) was held constant in this scenario and the hydraulic conductivity was varied in an attempt to calibrate the model. This resulted in a modeled hydraulic conductivity for the rock matrix and andesite sill layer of  $1.9 \times 10^{-7}$  m/s and  $1.9 \times 10^{-5}$  m/s, respectively. The transition zone was located between 740 to 1,560 mbsl, see Figure 3-2. Longitudinal dispersivity and transverse dispersivities were 120 and 10 m, respectively. The 200 and 32,800 mg/l isolines and the pathline from the working point of Long Shot can be seen in Figure A-8. The bump in the upper transition zone shown in the MT results for Long Shot located at approximately 1,000 m west of Long Shot was duplicated in the model. The dip of the upper transition zone that can be seen to the east in the MT results could not be duplicated. This dip is most likely due to other subsurface heterogeneities not yet included in the modeling effort. Freshwater discharges 30 m off shore on the Bering Sea coast. The transition zone ends 1,350 off shore-line. The ground water travel time from the working point of Long Shot is approximately 1,400 years. In the homogeneous minimum recharge scenario (scenario 1) the ground-water travel time was approximately 4,700 years. This shows that the ground water travel time changes significantly when an andesite sill layer is included in the subsurface. The hydraulic conductivity of the rock matrix is in the same order of magnitude as estimated by Gard and Hale (1964) and similar to the hydraulic conductivity that was simulated in the minimum recharge scenario (scenario 1), a decrease from  $2.3 \times 10^{-7}$  m/s to  $1.9 \times 10^{-7}$  m/s. The ground-water divide was at 890 m west of Long Shot which is approximately 250 m west of mid-island compared to only approximately 20 m as was modeled in the homogeneous minimum recharge scenario (scenario 1). A summary of the results for the andesite sill scenarios can be seen in Table 3-4.

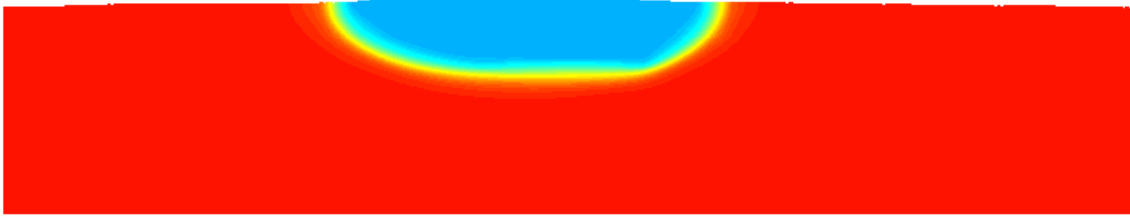


**Figure 3-2** Freshwater saltwater distribution of the Long Shot profile with an andesite sill layer located 1,000 m west and 1,000 m east of Long Shot. Hydraulic conductivities of the matrix rock and andesite sill were  $2.3 \times 10^{-7}$  m/s and  $2.3 \times 10^{-5}$  m/s respectively.

### Scenario 8

Similar to scenario 7, hydraulic conductivity was varied in this scenario while keeping the recharge constant ( $R_{max} = 3.13 \times 10^{-4}$  m/day). Hydraulic conductivity of the andesite sill and the matrix rock were chosen to  $7.3 \times 10^{-7}$  m/s and  $7.3 \times 10^{-5}$  m/s respectively in order for a transition zone at 700 to 1,600 mbsl to be modeled. Longitudinal and transverse dispersivities were the same as for scenario 7. The transition zone was located between 790 and 1,520 mbsl. Freshwater discharges at 30 m off shore-line in the Bering Sea and the transition zone ends at 1,500 m. The 200 and 32,800 mg/l isolines and the pathline from the working point of Long Shot can be seen in Figure A-9. Ground-water travel time is approximately 400 years. This is a decrease in ground-water travel time when compared to the homogeneous maximum recharge travel time of approximately 1,400 years. The hydraulic conductivity of the rock surrounding the sills is in the same order of magnitude as was estimated for the aquifer at the Long Shot site by Gard and Hale (1964) but decreased from  $7.9 \times 10^{-7}$  to  $7.3 \times 10^{-7}$  m/s when compared to the homogeneous maximum recharge scenario (scenario 2).

**Table 3-4** Simulation results from the scenarios with a layer of sill where measured values of recharge was given. Hydraulic conductivities (K), longitudinal and transverse dispersivities ( $\alpha_L$  and  $\alpha_T$ ) were changed until the location of the transition zone (TZ) was approximately between 700 to 1,600 mbsl.

	K (m/s)	$\alpha_L$ (m)	$\alpha_T$ (m)	TZ (mbsl)	Start of TZ distance from off- shore (m)	End of TZ from off- shore (m)	Travel time from LS to sea level (years)
<b>Scenario 7</b> ( $R_{sill}^{min}$ )	$1.9 \times 10^{-7}$	120	10	740 – 1,560	30	1,350	1,400
<b>Scenario 8</b> ( $R_{sill}^{max}$ )	$7.3 \times 10^{-7}$	120	10	790 – 1,520	30	1,500	400

### Summary of results from the andesite sill layer

The calibration of scenarios 7 and 8 resulted in a hydraulic conductivity of the rock matrix in the same order as estimated by Gard and Hale (1964). The freshwater discharges approximately 30 m to the east of the island for both scenarios 7 and 8. This is close to the modeled values for the homogeneous

scenarios. This result is also true for the location where the transition zone ends which was modeled to 1,350 and 1,500 m respectively for scenario 7 and 8. As for the shape of the upper transition zone shown in the MT results, the bump located at approximately 1,000 m west of Long Shot was the only feature that could be duplicated. Future modeling efforts will address other features of the shape of the upper transition zone. The ground-water travel time was determined to approximately 1,400 and 400 years for the minimum and maximum recharge, respectively. This is a significant decrease in travel time when compared to the homogeneous minimum and maximum scenarios (scenarios 1 and 2) showing the importance of modeling heterogeneities in the subsurface.

A summary of how well the modeled values fit to literature values can be seen in Table 3-5.

**Table 3-5** Summary of modeled results for the scenarios with an andesite sill layer and how they fit to literature values.

	<b>Constant parameter</b>	<b>Modeled parameter</b>	<b>In what order of magnitude modeled values fit to literature values</b>
<b>Scenario 7</b> ( $R^{min}_{sill}$ )	Recharge	Hydraulic conductivity	Same order of magnitude
<b>Scenario 8</b> ( $R^{max}_{sill}$ )	Recharge	Hydraulic conductivity	Same order of magnitude

#### 4. DISCUSSIONS AND CONCLUSIONS

Extensive geological and hydrological investigations were performed near the three sites: Cannikin, Milrow, and Long Shot before and after detonations. The ground-water modeling in this study was performed by using literature data from Gard and Hale (1964), U.S. Corps of Engineers and USGS (1965), Merritt and Fuller (1977). Furthermore, the model was calibrated to the magnetotelluric data measured at Amchitka in summer 2004. The transition zone of freshwater and saltwater was estimated between 700 to 1,600 mbsl at the Long Shot working point (Unsworth et al., 2005).

##### *Homogeneous*

Several scenarios were modeled by changing either the recharge or the hydraulic conductivity. The recharge to hydraulic conductivity ratio calculated from these simulations was  $4.56 \times 10^{-3}$ . This number is in the same order of magnitude as reported by Wheatcraft (1995) and DRI (2002) ( $6.9 \times 10^{-3}$  and  $6.3 \times 10^{-3}$  respectively). The dispersivities resulting from the calibration to MT results are similar to values used by Wheatcraft (1995) and DRI (2002). The minor differences are due to the location and thickness of the transition zone. In addition, Wheatcraft (1995) and DRI (2002) both estimated the annual precipitation to 1 m/year which is slightly higher than what was used in these simulations.

The parameters used in scenarios 1, 2, and 6 to calibrate the Long Shot model (permeability and recharge) are close to the values reported in the literature discussed in the previous section (see Table 3-3). Parameters used to calibrate scenarios 3, 4 and 5 do not compare well with literature values. Thus, scenarios 3, 4 and 5 should not be considered in further modeling.

Scenarios 1, 2, and 6 model a distance from shore to the end of the transition zone at approximately 1,360 m. The freshwater discharges 20 m off shore on the east side of the island for all modeled scenarios. Wheatcraft (1995) did not document where the freshwater discharge ended nor where the transition zone ended. An approximation was made from a figure presented in Wheatcraft (1995) in the report and which illustrated that the freshwater discharged at about 335 and that the transition zone ended at about 400 m. These distances were not documented by DRI (2002).

There are no reported values for porosity on Amchitka Island. Unsworth assumes a linear relationship between porosity and depth ranging from 0.3 at the surface and decreasing to 0.02 at a depth of 3000m. For the Long Shot ground water model a constant value for porosity of 0.1 was assumed. This value was selected from the results provided by Unsworth, which indicate that the porosity is approximately 0.1 at the depth of the Long Shot working point. Using this value for porosity will result in shorter estimated of travel time, since the porosity of the media above the working point will most likely be greater than 0.1 as indicated by Unsworth. The resulting ground water travel time for the Long Shot working point to the sea floor ranges between approximately 1,400 and 4,700 years for the most likely scenarios (scenarios 1,2 and 6) modeled. The shortest travel time was calculated in scenario 2, which used the maximum documented recharge and the longest travel time was for scenario 6 that used the higher range of hydraulic conductivity reported by Gard and Hale (1964).

Both Wheatcraft and DRI assumed the ground water divide at mid-island and, thus only modeled half the island. In scenario 1 ( $R_{\min}$ ) the ground water divide is shifted approximately 20 m to the east. This suggests that for a homogeneous island it should be sufficient to model only a half island and assume that the ground water divide is in the middle of the island.

It should be noted that these scenarios are assuming a homogeneous stratigraphy. This is most likely not the case. The following section examines the influence heterogeneity in hydraulic conductivity has on the ground water dynamics.

#### *Andesite sills influence on ground-water flow*

Due to time constraints only the minimum and maximum recharge scenarios were modeled with an added andesite sill layer. These two scenarios were chosen due to the most likelihood scenarios modeled in the homogeneous simulations. The hydraulic conductivity of the andesite sills was modeled as two orders of magnitude higher than the hydraulic conductivity of the rock matrix. In general it can be seen that when an andesite layer is added to the model, the

hydraulic conductivity of the rock matrix surrounding the sill is in the same order of magnitude as was chosen in the calibration for the homogeneous scenarios. This can be seen when comparing scenarios 1 and 7 and also when comparing scenarios 2 and 8. The results of the hydraulic conductivities are in the same order of magnitude as was estimated by Gard and Hale (1964) (see Table 3-5). The relatively more permeable layer of andesite will influence the travel time to the ocean from the working point of Long Shot. When an andesite sill layer was added to the minimum recharge scenario (scenario 1) the travel time decreased from approximately 4,700 to 1,400 years. This was also shown in the maximum recharge scenario where the travel time decreased from approximately 1,400 to 400 years.

The distance to where freshwater discharges in the Bering Sea and the distance to where the transition zone ends does not show a large difference when comparing the homogeneous scenarios with the andesite sills scenarios. It should be noted though that the east location of the upper transition zone (200 mg/l isolines) is not known but is indicated by the MT result to be further east than what has been modeled in these scenarios. This will need further study in order to locate the beginning and end of the transition zone at the Bering Sea side of Amchitka Island.

The location of the groundwater divide was at approximately 250 m west of the mid-island compared to only 20 m for the homogeneous minimum recharge scenario. Thus, when modeling heterogeneities of the island the whole island should be modeled rather than half island.

While these two scenarios show only preliminary results due to time constraints, they do suggest that the andesite sills do influence the ground-water dynamics. This result is noted when comparing the shape of the upper and lower boundaries of the transition zone generated in these modeling efforts to the results obtained from the MT survey of Long Shot. Most notable is the slight rise and subsequent dip to the west of the working point as well as the shift in the point of maximum depth in the lower boundary of the transition zone both shown in the inversion model for Long Shot (figure in MT results section) and in the modeled results. Future modeling efforts include and the third dimensions, which will include the faults on both sides of the Long Shot working point, adding additional subsurface features shown in the MT results, and adding the cavity and chimney to the model.



## APPENDIX A

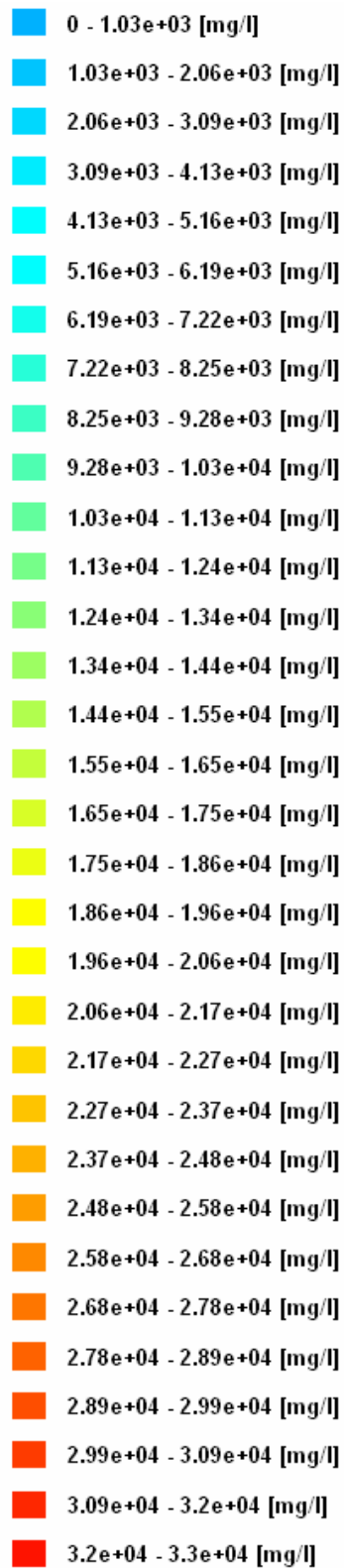
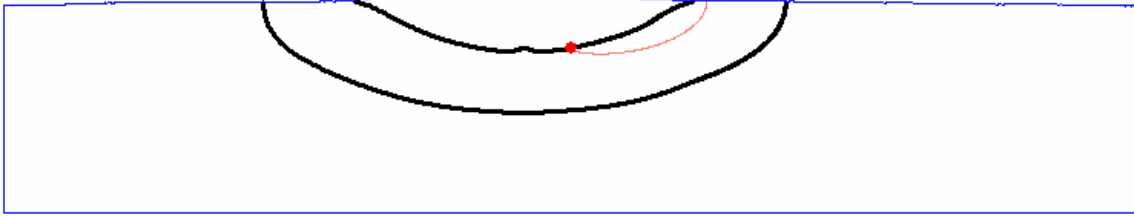
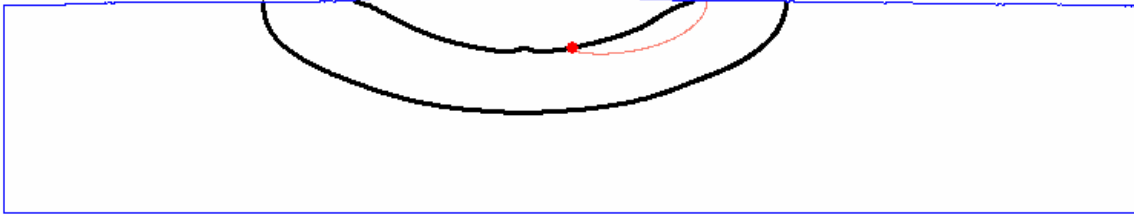


Figure A-1 Color legend for scenario 1.



**Figure A-2** Isolines 200 and 32,800 mg/l for scenario 1 ( $R_{\min}$ ) with Long Shot marked as a red circle. Illustrated is also a red pathline originating at the working point of Long Shot.



**Figure A-3** Isolines 200 and 32,800 mg/l for scenario 2 ( $R_{\max}$ ) with Long Shot marked as a red circle. Illustrated is also a red pathline originating at the working point of Long Shot.

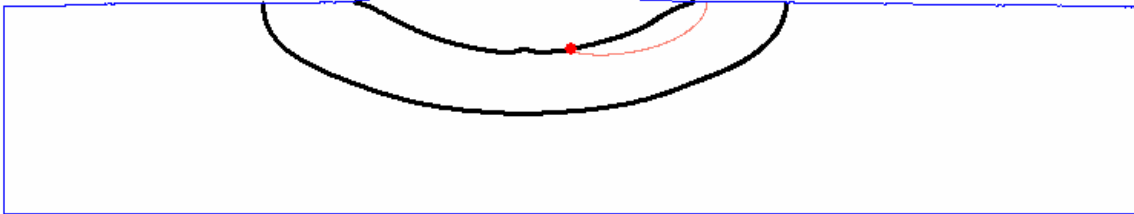


**Figure A-4** Isolines 200 and 32,800 mg/l for scenario 3 ( $K_{\text{Banjo}}$ ) with Long Shot marked as a red circle. Illustrated is also a red pathline originating at the working point of Long Shot.

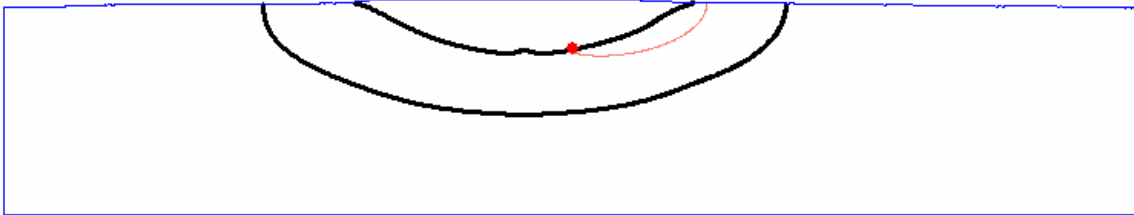


**Figure A-5** Isolines 200 and 32,800 mg/l for scenario 4 ( $K_{\text{Above sill}}$ ) with Long Shot marked as a red circle. Illustrated is also a red pathline originating at the working point of Long Shot.

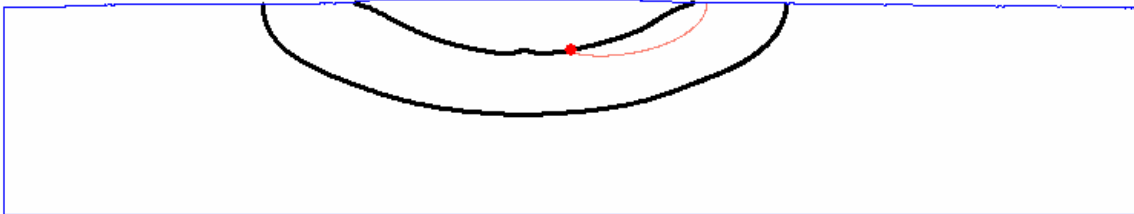


**Figure A-6** Isolines 200 and 32,800 mg/l for scenario 5 ( $K_{\text{LS}}^{\min}$ ) with Long Shot marked as a red circle. Illustrated is also a red pathline originating at the working point of Long Shot.

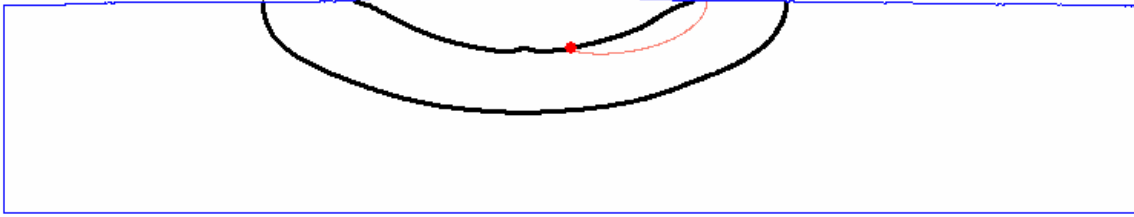


**Figure A-7** Isolines 200 and 32,800 mg/l for scenario 6 ( $K_{LS}^{max}$ ) with Long Shot marked as a red circle. Illustrated is also a red pathline originating at the working point of Long Shot.

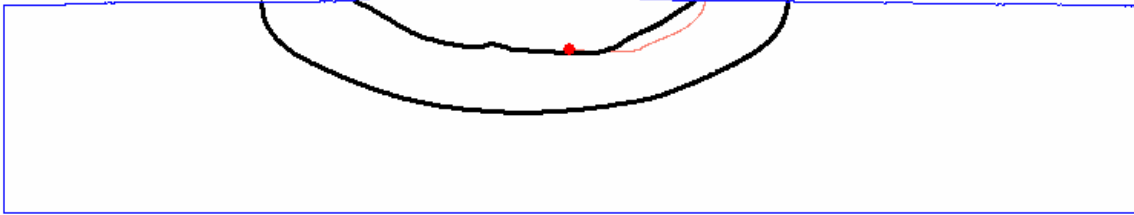


**Figure A-8** Isolines 200 and 32,800 mg/l for scenario 7 ( $R_{sill}^{min}$ ) with Long Shot marked as a red circle. Illustrated is also a red pathline originating at the working point of Long Shot.

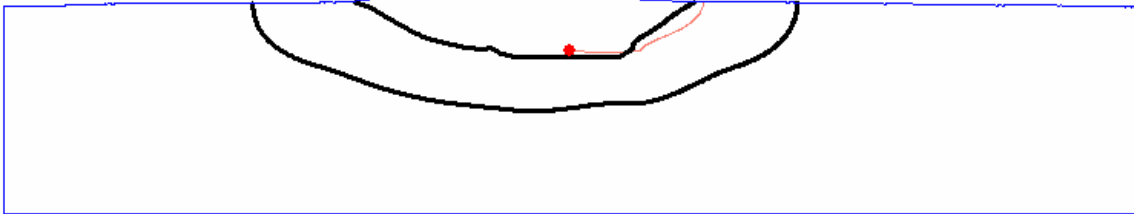


**Figure A-9** Isolines 200 and 32,800 mg/l for scenario 7 ( $R_{sill}^{max}$ ) with Long Shot marked as a red circle. Illustrated is also a red pathline originating at the working point of Long Shot.

## APPENDIX B

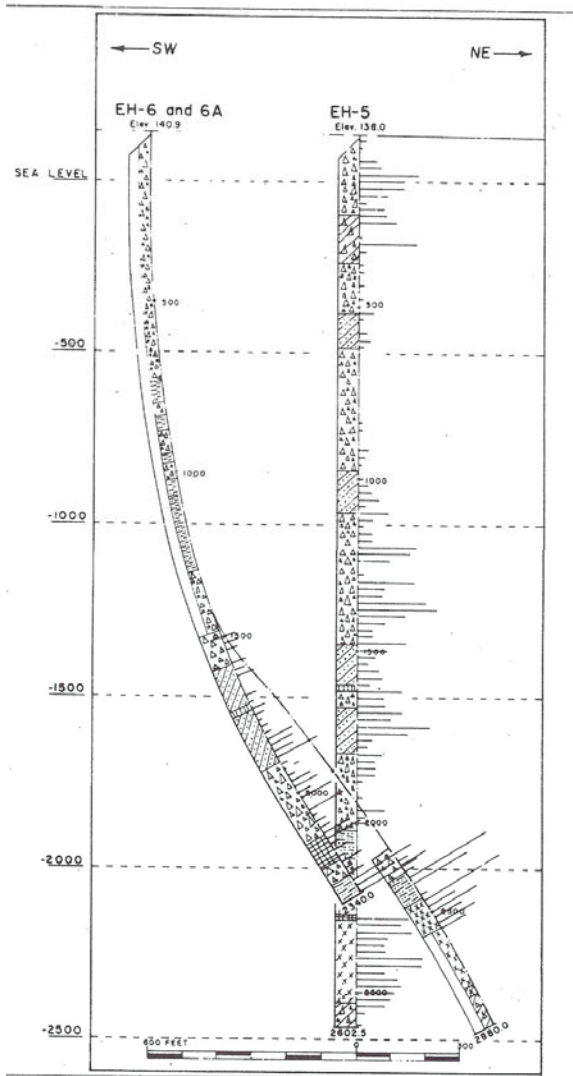


**Figure B-1** Joint frequencies for core hole EH-6, EH-6a, and EH-5.

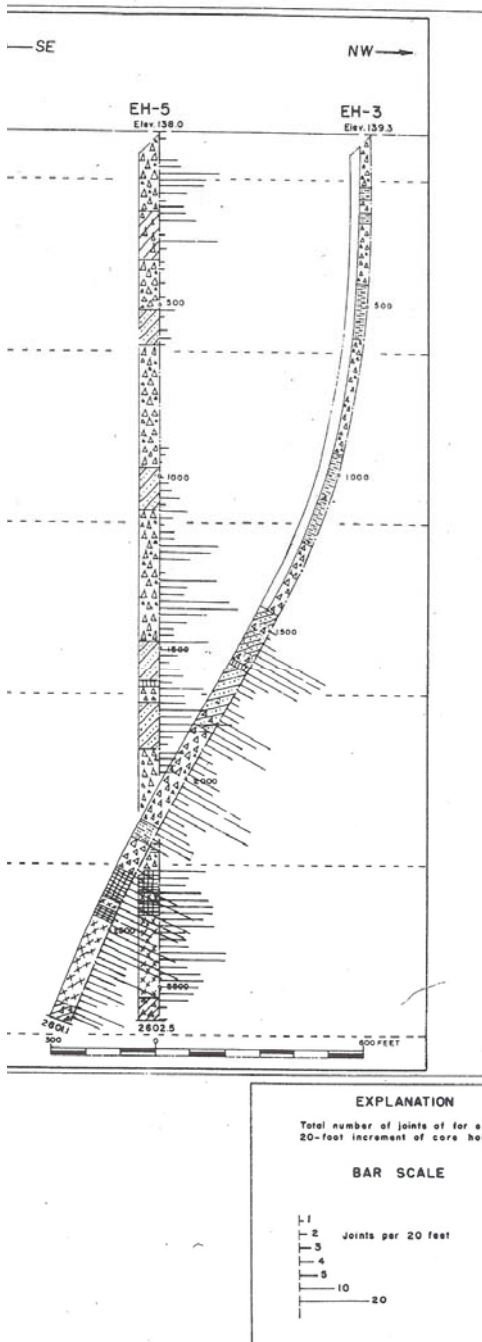


**Figure B-2** Joint frequencies for core hole EH-5, and EH-3.



## REFERENCES

- Carr, W.J., and W.D. Quinlivan, 1969. Progress report on the geology of Amchitka Island, Alaska, USAEC Report USGS-474-44, U.S. Geological Survey.
- Claassen, H.C., 1978. Hydrological processes and radionuclide distribution in a cavity and chimney produced by the Cannikin nuclear explosion, Amchitka Island, Alaska. U.S. Geological Survey, Professional Paper 712-D.
- DOE, 1997. Surface effects of Underground Nuclear Explosions. Department of Energy Report DOE/NV/11718-122.
- Earth Sciences Section Hazleton-Nuclear Science Corporation, 1964. Interim ground-water safety feasibility, project Long Shot.
- Fenske, 1972. Hydrology and radionuclide transport, Amchitka Island, Alaska. Desert Research Institute, Center for Water Resources Research, Report 45001, NVO-1253-1.
- Gard, L.M., and Hale, W.E., 1964. Technical Letter: Long Shot-1. Geology and hydrology of the Long Shot Site, Amchitka Island, Alaska. United States Department of the Interior Geological Survey.
- Gelhar, L.W., 1982. Analysis of two-well tracer tests with a pulse input. Report RHO-BW-CR-131 P, Rockwell International, Richland, Washington.
- Gonzalez, D. D., 1977. Hydraulic effects of underground nuclear explosions, Amchitka Island, Alaska. Ph.D. Dissertation, Colorado State University, Fort Collins, Colorado.
- Hassan A., K. Pohlmann, and J. Chapman (2002). Modeling groundwater flow and transport of radionuclides at Amchitka Island's underground nuclear tests: Milrow, Long Shot, and Cannikin. Desert Research Institute No. 45172.
- Hazleton-Nuclear Science Corporation, 1964. Interim ground-water safety feasibility, project Long Shot. Earth Sciences Section Hazleton-Nuclear Science Corporation Palo Alto, California. HNSTR-1229-123.
- Johnson, M., et.al. 2005. Results from the Amchitka Oceanographic Survey. CRESF
- Merritt, M.L., and R.G. Fuller, editors, 1977. The environment of Amchitka Island, Alaska. Energy Research and Development Administration, Technical Information Center.
- Perret, W.R. and D.R. Breeding, 1972. Ground motion in the vicinity of an underground nuclear explosion in the Aleutian Islands: Milrow event. Sandia Laboratories SC-RR-71 0668.
- Perry, R.B., and H. Nichols, 1965. Bathymetry of Adak Canyon, Aleutian Arc, Alaska. Geological Society of America Bulletin, v. 76, no.3.
- Robertson, J.B., 1974. Digital modeling of radioactive and chemical transport in the Snake River Plain aquifer of the National Reactor Testing Station, Idaho, U.S. Geological Survey. Open file report IDO-22054.
- SRTM, 2005. <http://srtm.usgs.gov/>

- Unsworth, M., W. Soyer, V. Tuncer, 2005. Magnetotelluric measurements for determining the subsurface salinity and porosity structure of Amchitka Island, Alaska. CRESP.
- U.S. Army Corps of Engineers and U.S. Geological Survey, 1965. Project Long Shot Amchitka Island, Alaska, Geologic and Hydrologic Investigations (Phase 1). Unnumbered report.
- US Geological Survey, 1970. Geologic and hydrologic effects of the Milrow event, Aleutian Islands, Alaska. U.S., Geological Survey Report USGS 474-71.
- US Geological Survey, 1972. Geologic and hydrologic effects of the Cannikin underground nuclear explosion, Amchitka Island, Aleutian Islands, Alaska. U.S., Geological Survey Report USGS 474-148.
- Gonzalez, D. D. et al, 1974.. Bathymetry of Cannikin Lake, Amchitka Island, Alaska, with an evaluation of computer-mapping techniques. U.S, Geological Survey Report USGS-474-203.
- Wheatcraft, S.W., 1995. Sea water intrusion model of Amchitka Island, Alaska. Nevada Operations Office, U.S. Department of Energy Report DOE/NV/10845-59.